JVI Journals.ASM.org

Implication of *Bemisia tabaci* Heat Shock Protein 70 in Begomovirus-Whitefly Interactions

Monika Götz,[a] Smadar Popovski,[b] Mario Kollenberg,[a] Rena Gorovits,[c] Judith K. Brown,[d] Joseph M. Cicero,[d] Henryk Czosnek,[c] Stephan Winter,[a] and Murad Ghanim[b]

Leibniz Institute DSMZ-German Collection of Microorganisms and Cell Cultures, Plant Virus Department, Braunschweig, Germany[a]; Department of Entomology, Volcani Center, Bet Dagan, Israel[b]; Institute of Plant Sciences and Genetics in Agriculture, Robert H. Smith Faculty of Agriculture, Food and Environment, Hebrew University of Jerusalem, Rehovot, Israel[c]; and School of Plant Sciences, University of Arizona, Tucson, Arizona, USA[d]

The whitefly *Bemisia tabaci* (Gennadius) is a major cosmopolitan pest capable of feeding on hundreds of plant species and transmits several major plant viruses. The most important and widespread viruses vectored by *B. tabaci* are in the genus *Begomovirus*, an unusual group of plant viruses owing to their small, single-stranded DNA genome and geminate particle morphology. *B. tabaci* transmits begomoviruses in a persistent circulative nonpropagative manner. Evidence suggests that the whitefly vector encounters deleterious effects following *Tomato yellow leaf curl virus* (TYLCV) ingestion and retention. However, little is known about the molecular and cellular basis underlying these coevolved begomovirus-whitefly interactions. To elucidate these interactions, we undertook a study using *B. tabaci* microarrays to specifically describe the responses of the transcriptomes of whole insects and dissected midguts following TYLCV acquisition and retention. Microarray, real-time PCR, and Western blot analyses indicated that *B. tabaci* heat shock protein 70 (HSP70) specifically responded to the presence of the monopartite TYLCV and the bipartite *Squash leaf curl virus*. Immunocapture PCR, protein coimmunoprecipitation, and virus overlay protein binding assays showed *in vitro* interaction between TYLCV and HSP70. Fluorescence *in situ* hybridization and immunolocalization showed colocalization of TYLCV and the bipartite *Watermelon chlorotic stunt virus* virions and HSP70 within midgut epithelial cells. Finally, membrane feeding of whiteflies with anti-HSP70 antibodies and TYLCV virions showed an increase in TYLCV transmission, suggesting an inhibitory role for HSP70 in virus transmission, a role that might be related to protection against begomoviruses while translocating in the whitefly.

Tomato yellow leaf curl virus (TYLCV) is a complex of single-stranded-DNA plant viruses of the genus *Begomovirus* in the family *Geminiviridae* that causes severe damage in tomatoes by stopping or interfering with normal plant growth, thus significantly affecting crop yields. Begomoviruses exhibit tissue tropism in the plant phloem, and some are effectively transmitted by phloem feeders, such as the whitefly *Bemisia tabaci* (17, 18). TYLCV is transmitted exclusively by *B. tabaci*, and many of the parameters for acquisition, transmission, and retention of the virus by *B. tabaci* have been studied in depth (10, 11, 55, 68); however, the molecular interactions that underlie the persistence of the virus in its vector are unknown for the most part. TYLCV is transmitted by *B. tabaci* in a persistent circulative nonpropagative manner (31); however, it has been shown that virus genes may be transcribed in the whitefly vector (70). TYLCV is ingested by *B. tabaci* with the phloem sap, passes through the food canal in the stylet, reaches the chitin-lined esophagus in the thorax, and enters the filter chamber which connects the midgut with the hindgut (28, 29). The majority of TYLCV particles are absorbed into the hemolymph in the filter chamber (16, 25, 71), while some move along the descending and ascending midgut and are also absorbed by midgut epithelial cells. Virus particles circulate in the hemolymph and reach the salivary glands, where they are internalized into the primary salivary glands, move along the salivary duct, and are injected with the saliva back into the plant phloem (13, 16, 28, 29, 39). Interaction of TYLCV with the insect is mediated by the coat protein (CP) of the virus. CP is thought to be the only viral protein required for insect-mediated transmission (3, 8, 36, 62).

The intimate relationships between the virus and *B. tabaci* suggest an active molecular response of whitefly genes and proteins to the presence of the virus. These relationships include association of TYLCV with the entire life of the B biotype of *B. tabaci* (recently termed Middle East-Asia Minor 1 (MEAM1) (19, 21, 68). This long-term association was correlated with a decrease in longevity and fertility of the insect (68). Similar results were obtained with a TYLCV isolate from China (*Tomato yellow leaf curl China virus* [TYLCCV]) in two *B. tabaci* cryptic species, MEAM1 and Asia II 2 (40). TYLCV was shown to be transovarially transmitted to the progeny of viruliferous whiteflies, and the viruliferous progenies were able to transmit the virus to tomato test plants (31). Similar results were obtained with *Tomato yellow leaf curl Sardinia virus* (TYLCSV); however, the transmission occurred to one generation, and the progenies were unable to transmit the virus to test plants (7). TYLCV was also shown to be transmitted from viruliferous males to nonviruliferous females and vice versa through mating, and again the individuals that received the virus via mating were able to transmit the virus to tomato test plants (30).

During the translocation of begomoviruses in the whitefly, it is likely that they interact with proteins that facilitate transport from the digestive tract to the hemolymph and from the hemolymph to

Received 7 April 2012 **Accepted** 11 September 2012
Published ahead of print 26 September 2012
Address correspondence to Murad Ghanim, ghanim@volcani.agri.gov.il.
This is contribution 508/12 from the ARO, The Volcani Center, Bet Dagan, Israel.
Supplemental material for this article may be found at http://jvi.asm.org/.

doi:10.1128/JVI.00880-12

the salivary glands. These interactions may induce innate immunity and stress-responsive whitefly genes. To date, only a small number of proteins were shown to be indirectly involved in the transmission of begomoviruses. Similar to the peach potato aphid *Myzus persicae-Potato leafroll virus* system, a 63-kDa GroEL protein produced by endosymbionts of *B. tabaci* was shown to be involved in TYLCV transmission by *B. tabaci* (37, 56, 57, 77, 78). This protein is abundant in the hemolymph of the insect and exhibits binding affinity for TYLCV (56). It has been shown that feeding whiteflies with anti-GroEL antiserum prior to acquisition of virions reduced TYLCV transmission by more than 80%. It has also been shown that TYLCV particles that reach the hemolymph interact with GroEL on their way to the salivary glands, forming a complex that protects virions from rapid proteolysis (56). Immunogold labeling with anti-GroEL antibodies suggested that this GroEL is produced by a secondary symbiont in bacteriosomes of *B. tabaci* MEAM1 (57). This GroEL protein was shown to be produced by the secondary symbiont *Hamiltonella* in *B. tabaci* MEAM1, thus making this species a much more efficient vector for TYLCV than *B. tabaci* Mediterranean (MED), which does not harbor *Hamiltonella* (32). Only a small number of nonbacterial proteins were shown to be indirectly involved in the transmission of begomoviruses. In order to search for such proteins, the CP was used as bait in a yeast two-hybrid screen against a cDNA library constructed from *B. tabaci* MED, formerly known as the Q biotype (19, 21), to search for proteins interacting with the virus (64). While very few responsive proteins were identified, only a 16-kDa small heat shock protein (named BtHSP16) belonging to the HSP20/alpha crystallin family was shown to bind to the TYLCSV CP and identified as good candidate for involvement in virus translocation.

A recent study profiled the response of *B. tabaci* MEAM1 to the presence of TYLCV from China (TYLCCV), using a whole-transcriptome approach. One thousand six hundred six genes were significantly regulated in viruliferous whiteflies. These genes were involved in 157 biochemical pathways, including cell cycle, primary metabolism, activation of the whitefly immune responses, and induction of the autophagy mechanism in ovaries and fat bodies (47). TYLCCV also suppressed whitefly Toll-like and mitogen-activated protein kinase (MAPK) pathways, which are involved in immune responses.

In this study, *B. tabaci* DNA microarrays were used to search for genes that respond to the acquisition and retention of TYLCV in *B. tabaci* MEAM1. Among the several responsive genes identified, we found that a heat shock 70 gene (*hsp70*) specifically responds to the acquisition and retention of two begomoviruses that were tested. Several *in vitro* and *in vivo* experiments confirmed the specific interaction of the virus with HSP70. These results suggest that the expression of *hsp70* is induced in *B. tabaci* as a protective response to TYLCV. This overexpression seems to have a role in reducing the deleterious effect of the virus, since anti-HSP70 antibody feeding leads to an increase in TYLCV transmission by *B. tabaci*.

MATERIALS AND METHODS

Maintenance of viruses and synchronization of whitefly population. Experiments were conducted in two locations: Volcani Center in Israel and Leibniz Institute-DSMZ German Collection of Microorganisms and Cell Cultures in Germany. In Israel, all *B. tabaci* populations used were reared on cotton plants (*Gossypium hirusutum* cv. Akala) grown in insect-proof cages at 26°C ± 2°C. The populations of the MEAM1 (Middle East-Asia Minor 1, formerly biotype B [21, 24]) used in this study harbored the primary symbiont *Portiera* and the secondary symbionts *Hamiltonella* and *Rickettsia.* In Germany, *B. tabaci* MEAM1 was used and kept under the same rearing conditions and harbored the symbiotic bacteria *Portiera* and *Hamiltonella* and the secondary endosymbiont *Wolbachia*. All experiments were conducted in insect-proof cages kept at 26°C ± 2°C in an insect-proof growth chamber. The whiteflies used in all experiments were synchronized 4 to 7 days after emergence and were used for maintaining the virus by whitefly-mediated transmission from infected to healthy plants. After 3 to 4 weeks, the plants were visually monitored for the appearance of disease symptoms, and DNA was extracted (20) and subjected to PCR and dot blot analyses to detect the presence of the virus (31). For virus overlay protein binding assays, whiteflies were collected once a week by aspiration and stored at −80°C until protein extraction.

RNA isolation and cDNA synthesis. Whiteflies were collected and homogenized in TRI reagent (MRC Inc., Cincinnati, OH). All samples were treated with RQ1 DNase (RNase free) (Promega Corporation, Madison, WI) to avoid DNA contamination. The RNA served as a template for reverse transcription reactions in a reverse transcription-PCR (RT-PCR) approach and for linear amplification (4) for labeling in microarray hybridizations. Oligo(dT) primer served for first-strand synthesis. For microarrays, whiteflies were given an acquisition access period for 48 h on TYLCV-infected tomato plants and then were transferred to cotton non-TYLCV-host plants for 3 days for clearing the effect of the infected plant on gene expression. As a control, whiteflies were reared on healthy tomato plants and then cotton plants for the same periods of time. Total RNA was isolated from 100 adult female whiteflies that had acquired the virus and from 100 control whiteflies. The same was also done from 100 heads with the first segment of the thorax (to include the salivary glands) and 125 dissected midguts and their control counterparts. Each of these RNA preparations was replicated three times. Microarray methods and data analyses are given in File S1 in the supplemental material.

qRT-PCR analysis. To verify the enhanced expression of the *hsp70* gene, a quantitative RT- PCR (qRT-PCR) approach was used. The primer pair used for the amplification is 5′-ACTCCGACAATCAACCTGGT-3′ for the forward primer and 5′-TCCCGAGGAGATTGTTGTCC-3′ for the reverse primer, with a predicted product size of 81 bp. Actin was used as a normalization gene with the forward primer 5′-TCTTCCAGCCATCCTTCTTG-3′ and the reverse primer 5′-CGGTGATTTCCTTCTGCATT-3′ with an expected product size of 81 bp. Amplifications were performed using 1× Quantitect SYBR green PCR mix (Qiagen, Hilden, Germany) and 5 pmol of each primer. To ensure the validity of the data, the expression of each gene was tested in triplicate in each of three biologically independent experiments. Each RNA sample in each replicate was prepared from 50 individuals. The cycling conditions were as follows: 15 min of activation at 95°C and 45 cycles of 10 s at 95°C, 20 s at 60°C, and 25 s at 72°C. A melting ramp from 60°C to 99°C was used, with a 1°C rise at each step, waiting 5 s between steps. The channel source was 470 nm, with a detector at 510 nm. A Rotor-Gene 6000 machine (Corbett Robotics Pty. Ltd., Brisbane, Australia) and the accompanying software were used for qPCR data normalization and quantification. Average expression of actin cDNA, which was not regulated after the virus acquisition experiments, was used as a reference as stated above.

HSP70 and TYLCV CP coimmunoprecipitation. For immunoprecipitation, protein A-Sepharose beads (Pharmacia) were incubated with an excess of either anti-CP or anti-HSP70, or their corresponding preimmune serums as controls, in binding buffer (50 mM Tris-HCl [pH 7.5], 150 mM NaCl, 2 mM EDTA, and 0.5% NP-40) for 2 h at 4°C. After unbound antibodies were removed, whitefly soluble protein extracts were added and incubated for 10 h at 4°C. Immunoprecipitated proteins were eluted by boiling in PAGE buffer. Each immunodetection was repeated at least three times. Incubation with antibodies was followed by ECL detection (Amersham, United Kingdom). Protein A-Sepharose beads bound to

anti-GroEL antibody were used to show a lack of interaction between HSP70 and GroEL as a negative control.

Immunodetection of HSP70 and virus overlay protein binding assays. To extract soluble and insoluble proteins from whiteflies, frozen insects were homogenized in ice-cold protein extraction buffer (100 mM Tris-HCl, 1 mM EDTA, 1.5% glycerol, 1% Triton X-100, and 1% proteinase inhibitor mix M [Serva Electrophoresis GmbH, Heidelberg, Germany]) with a cordless motor (VWR, Darmstadt, Germany) and spun for 30 min at 14,000 × *g* at 4°C. The supernatant was collected, and extraction was repeated. Supernatants were combined and referred to as soluble protein fraction. The pellet was washed twice with extraction buffer. The proteins of the soluble protein fraction and the pellet were precipitated with ice-cold acetone overnight. After 20 min of centrifugation at 14,000 × *g* and 4°C, the acetone was discharged and the pellets were dried in a speed vacuum concentrator (Speed Vac SC 110; Thermo Fisher Scientific GmbH, Schwerte, Germany) for 2 min. The proteins were solved in extraction buffer, and protein concentration was determined using a 2-D Quant kit (GE Healthcare, Freiburg, Germany).

SDS electrophoresis and electrotransfer of proteins. A total of 80 μg insect protein per lane was loaded on an SDS-polyacrylamide gel (15%) and separated at a constant 140 V (Hoefer mini VE vertical electrophoresis system; Hoefer Scientific Instruments, San Francisco, CA). Identical gels were run for Coomassie staining, Western analysis, and virus overlay protein binding assays. After electrophoresis, proteins were either fixed (10% acetic acid and 40% ethanol) and stained with colloidal Coomassie brilliant blue (Sigma-Aldrich, Munich, Germany) or were transferred onto nitrocellulose membranes (0.2 μm, Whatman Protran BC 83; Whatman GmbH, Dassel, Germany) at 350 mA for 2 h in ice-cold Towbin buffer (25 mM Tris [pH 8.3], 192 mM glycine, 15% methanol, and 0.1% SDS) for Western analysis and virus overlay protein binding assays (Hoefer mini VE electrotransfer unit). Nitrocellulose blots were stained with Ponceau S solution (Serva Electrophoresis GmbH, Heidelberg, Germany), and the positions of visible protein bands were recorded by scanning. After the stain was stripped with TBS buffer (10 mM Tris-HCl [pH 7.5], 150 mM sodium chloride), the membranes were blocked with skimmed milk (5%) in TBS buffer at 4°C overnight.

Western blot immunodetection of HSP70 and tubulin. Blocked membranes were incubated with mouse monoclonal antibody against HSP70 (diluted 1:1,000 in TBS buffer, ab74072; Abcam, Cambridge, United Kingdom) for 1 h and after intensive washing with rabbit anti-mouse IgG-alkaline phosphatase (AP) (1:5,000 in TBS; Dako, Cytomantion GmbH, Hamburg, Germany) for 45 min. The detection of HSP70 was done after application of 5-bromo-4-chloro-3-indolylphosphate–nitroblue tetrazolium (BCIP-NBT) (Promega Corporation, Madison, WI). Detection of tubulin followed the same protocols using a rat monoclonal antibody (diluted 1:1,000 in TBS buffer, ab6160; Abcam, Cambridge, United Kingdom) and a respective secondary antibody conjugated to AP.

Virus overlay protein binding analysis (VOPBA). Blocked membranes were incubated with purified virus particles of TYLCV and *Yam sphaerical aureus virus* (YSV), as described in File S1 in the supplemental material (40 μg per ml in TBS buffer), overnight at 4°C. Control blots were incubated with TBS buffer without virions. After washing, membranes were incubated with the primary antibodies DSMZ AS-546/1 (1 μg ml^{-1} in TBS; 4 h) for the detection of TYLCV and DSMZ AS-517 (1 μg ml^{-1} in TBS, 2 h) for YSV. Virus-antibody complexes were visualized after incubation with alkaline phosphatase-conjugated rabbit anti-mouse IgG (1:5,000 in TBS; 10 mM Tris-HCl [pH 7.5] and 150 mM NaCl; Dako, Cytomantion GmbH, Hamburg, Germany) and goat anti-rabbit IgG-AP (1:30,000 in TBS; Sigma-Aldrich, Munich, Germany), respectively, and BCIP-NBT color development substrate (Promega Corporation). All detection steps were performed at room temperature with rocking. The reaction was stopped when bands had developed. Membranes were scanned and compared to the Ponceau S images, and protein bands corresponding to the virus binding bands on the membranes were selected in the Coomassie stained gels, picked, and analyzed by electrospray ionization mass spectrometry (ESI-MS) (Henning Urlaub, Bioanalytical Mass Spectrometry, Max Planck Institute for Biophysical Chemistry, Göttingen, Germany). Peptide mass spectra were analyzed using the software program Scaffold3 (Matrix Science).

IC-PCR. Interaction between HSP70 and TYLCV was detected by immunocapture-PCR assay (IC-PCR) (32). The buffers used for IC-PCR are described by the manufacturer (Bioreba, Ebringen, Germany) and were used as instructed by the manufacturer. PCR tubes were filled with 200 μl of anti-HSP70 antiserum (1:1,000-diluted in coating buffer), incubated for 3 h at 37°C, and washed five times for 5 min (each time) with 200 μl washing buffer. Homogenates from 30 to 40 whiteflies caged with TYLCV-infected tomato plants for 48 h were incubated for 18 h at 4°C in the coated PCR tubes in 200 μl of extraction buffer. The tubes were washed five times, 5 min each time, with 200 μl washing buffer and dried. PCR amplification of the viral DNA from the virions bound to the HSP70 protein, which was itself bound to the antibody-coated tubes, was performed with the TYLCV-specific primers V61 and C473 (31). All experiments were replicated 3 to 5 times.

Transmission of TYLCV after feeding on HSP70 antibodies. To assess the implication of HSP70 in the transmission of TYLCV, synchronized 5- to 8-day-old whiteflies were fed on antibodies against HSP70 (1:200, ab310010; Abcam, Cambridge, United Kingdom) in 15% sucrose solution through Parafilm M (Brand GmbH + Co, Wertheim, Germany). After 1 day, the medium was replaced by a sucrose solution containing purified TYLCV particles (10 μg ml^{-1}) and HSP70 antibodies (1:200), and whiteflies were fed for another day. Whiteflies fed on preimmune serum (1:200) in 15% sucrose solution following preimmune serum (1:200) in 15% sucrose solution containing TYLCV virions (10 μg ml^{-1}) served as a control. Subsequently, single whiteflies were transferred to tomato plants (2- to 3-leaf stage) and incubated in Plexiglas tubes under greenhouse conditions for 7 days. The whiteflies that were incubated with the plants were tested for the presence of TYLCV by PCR, and only plants that were caged with whiteflies that tested positive for TYLCV were used for disease symptom monitoring after 28 days postinoculation. Symptomless tomato plants were tested for TYLCV infection by PCR. The experiments were performed twice with 26 plants for each treatment.

Detection of HSP70 antibodies after feeding on antibody-amended sucrose solution. The ingestion of HSP70 antibodies was proven as described previously by Morin et al. (57) with modifications. Whiteflies were collected 5 to 8 days after emergence and were fed on a sucrose solution amended with HSP70 antibodies or preimmune serum as control for 2 days (as described for the transmission of TYLCV after antibody feeding). After 4 h of starvation, whiteflies were frozen and homogenized in ice-cold TBS buffer with a cordless motor. Homogenates were used as primary antibodies. Protein blots of soluble and insoluble whitefly proteins (80 μg protein per lane) were incubated with the whitefly homogenates or with HSP70 antibodies (1:200 in TBS, ab310010; Abcam) for 20 h at 4°C and after washing with the secondary antibodies goat anti-rabbit IgG-AP (1:30,000 in TBS; Sigma-Aldrich, Munich, Germany) for 1 h. The detection was done after application of BCIP-NBT. For *in situ* detection of the ingested antibody in the midgut, whiteflies were fed with the first anti-HSP70 antibody for 24 h from artificial diet or with preimmune serum in the control group and then were fed with a goat-anti rabbit Alexa Fluor 568-nm secondary antibody diluted 1:100 for additional 24 h. Midguts were dissected from both groups, whole mounted in 1× phosphate-buffered saline (PBS) solution containing 1 μl of 10 mg ml^{-1} 4′,6-diamidino-2-phenylindole (DAPI) solution, and viewed under an IX81Olympus FluoView500 confocal microscope.

Additional methods are given in File S1 in the supplemental material.

RESULTS

Microarray results. The transcriptional response of *B. tabaci* MEAM1 female adults that had acquired and retained the two begomoviruses TYLCV and SLCV was investigated using DNA microarrays. The overall microarray results clearly indicated a transcriptional response after virus acquisition and retention. The

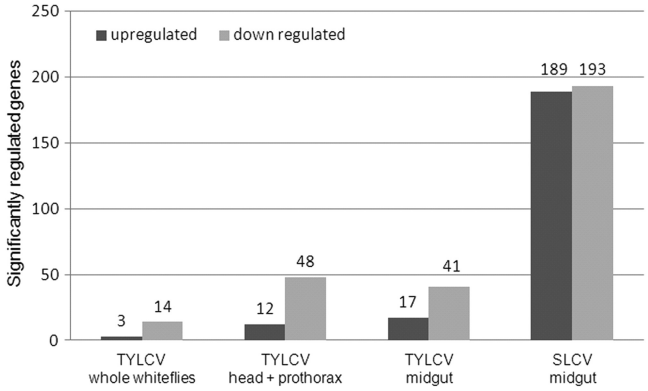

FIG 1 Significantly induced (black) and repressed (gray) genes based on their fold change in expression in the microarray experiments following the acquisition of either TYLCV or SLCV. Analyzed samples were whole whiteflies, head-prothorax, and midguts for TYLCV and midguts for SLCV.

transcriptional response of *B. tabaci* to TYLCV was not pronounced, and only a low number of genes responded to the presence of the virus. Overall, 14 genes were downregulated and 3 genes were upregulated when whole whiteflies were analyzed. However, proportionally more genes were significantly regulated from head-prothorax (12 up- and 48 downregulated) and from dissected midguts (17 up- and 41 downregulated) than was the case for whole whiteflies, suggesting a masking effect when whole whiteflies were analyzed (Fig. 1). Taking the fact that the number of genes regulated from the midgut was greater than the number of regulated genes from whole whiteflies, we analyzed the response of *B. tabaci* females to another begomovirus, SLCV. Surprisingly, a much higher number of midgut genes were significantly regulated in response to this virus, with 189 upregulated and 193 downregulated genes (Fig. 1). The regulated genes were examined for their fold change in expression and possible functional relevance to virus translocation, macromolecule movement, defense or stress response, and other functions that might be relevant to the acquisition and retention of the viruses (Table 1). The response of the

TABLE 1 Differentially transcribed ESTs in the midgut of *B. tabaci* following TYLCV and SLCV acquisition and retention[a]

EST clone	Best hit in GenBank	GenBank accession no.	GO term	Biological function	Microarray expression in midgut	
					TYLCV	SLCV
HBT008_F09_T3_078	70-kDa heat shock	EE597405	000940	Response to heat, protein folding	1.65	1.51
TOMOV-BT003_A05	OS-D-like	EE599211	0009700	Sensory perception	2.81	
BT-H-034-1-H5-T3_H05	Pantothenate kinase 4	EE596485	0015937	Coenzyme A biosynthesis		5.74
BT-H-032-1-C9-T3_C09	Transmembrane assembly	EE596401	0006928	Cellular component movement		3.96
BT-TYLCV-053-1-H9-T3_H09	Checkpoint-like	EE601807	0000075	Cell cycle checkpoint		3.22
BT-H-020-1-E2-T3_E02	Cathepsin B protease	EE595866	000691	Autophagy, proteolysis response to stress		2.09
BT-TYLCV-018-1-H4-T3_H04	Sugar transporter	EE600420	000535	Glucose transmembrane transporter		2.01
BT-TOMOV-040-1-G8-T3_G08	Btk-1	EE598908		Immunity		1.59
HBT006_G06_T3_051	Cathepsin F protease	EE597298	000658	Proteolysis, receptor-mediated endocytosis		1.59
BT-TYLCV-056-1-F6-T3_F06	ATP synthase	EE601889	0042776	ATP synthesis-coupled proton transport	-1.7	-2.6
BT-TOMOV-042-1-F9-T3_F09	NADH dehydrogenase subunit 1	EE599001	0005747	Mitochondrial respiratory chain complex I		2.7
BT-TYLCV-057-1-E4-T3_E04	Nuclear envelope membrane protein	EE601922	001503	Transmembrane transport		2.58
BT-TYLCV-051-1-A8-T3_A08	Fatty acid binding protein	EE601683	000521	Transporter activity		1.97
TOMOV-BT012_G05	Sugar transporter	EE599789	000535	Glucose transmembrane transporter activity		2.01
BT-HINST-004-1-C2-T3_C02	ATP synthase subunit C	EE602876	0040007	Cytoplasmic membrane-bounded vesicle		1.88
TOMOV-BT012_C02	Phosphoglycerate mutase 1	EE599756	0006096	Glycolysis		1.55
BT-TYLCV-045-1-A6-T3_A06	Cytochrome *c* oxidase subunit III	EE601430	0006123	Mitochondrial electron transport		1.55
BT-TOMOV-028-1-A9-T3_A09	Adenine nucleotide translocator	EE598307	0055085	Transmembrane transport		1.54
BT-TYLCV-042-1-B2-T3_B02	ATP-binding FecE	EE601334	0006811	Ion transport		1.53
BT-TYLCV-018-1-H4-T3_H04	Acyl-coenzyme A esterase	EE600420	0004091	Protein binding		2.01
BT-TYLCV-051-1-A8-T3_A08	Putative fatty acid binding protein	EE601683	000521	Transporter activity		1.97
TOMOV-BT012_C02	Phosphoglycerate mutase 1	EE599756	0006096	Glycolysis		1.55
BT-TOMOV-020-1-D2-T3_D02	Vitellogenin	EE597946	0006869	Lipid transport		1.67
TYLCV006_F04	Cytochrome P450 CYP6CX2	EE602200	0055114	Oxidation reduction	1.78	
BT-TYLCV-058-1-F5-T3_F05	Cytochrome oxidase I	EE601978	000612	Mitochondrial electron transport	−1.78	
BT-TOMOV-028-1-E7-T3_E07	Sodium-dependent glucose transporter	EE598330	000864	Carbohydrate transport	−1.63	
BT-HINST-020-1-B11-T3_B11	Apolipophorin III	EE603648	0008289	Lipid binding	−1.69	
BT-TYLCV-025-1-B7-T3_B07	Cytochrome *c* oxidase subunit II	EE600708	000609	Precursor metabolites and energy	−1.57	

[a] EST (expressed sequence tag) clone name, best hit in GenBank, GenBank accession no. of the EST, GO (gene ontology) category, biological function of the expected protein, and the average ratio of three highly correlated biological replicates following the microarray experiments comparing viruliferous and nonviruliferous midguts with TYLCV or SLCV are shown.

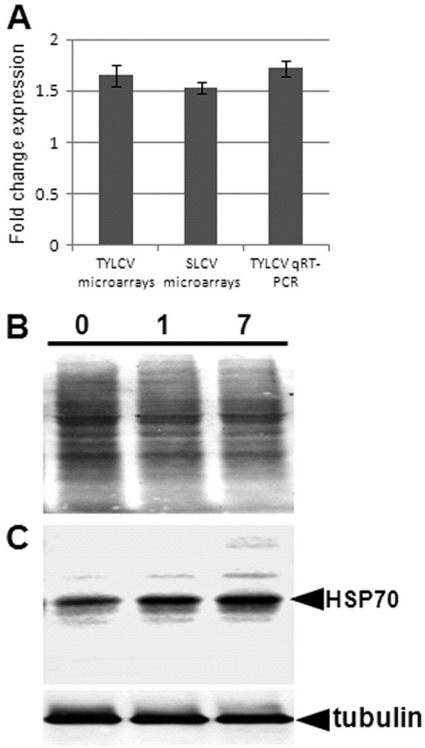

FIG 2 (A) Fold change in overexpression of *hsp70* in viruliferous whiteflies, calculated after microarray and qRT-PCR analyses. Both analyses were further performed with nonviruliferous whiteflies, and the qRT-PCR results were normalized to the expression of an actin gene. (B and C) Increase in the HSP70 concentration after acquisition of TYLCV. Total proteins were extracted from whole whiteflies after virus acquisition and retention for 0, 1, and 7 days, subjected to SDS-PAGE (B), and blotted and incubated with HSP70-specific antibodies to follow the HSP70 levels over time (C). The expression of *B. tabaci* tubulin did not change following virus acquisition and retention and is given as a loading control.

genes was not high as measured by their fold change in expression. The majority of the genes showed downregulation with TYLCV, while in the case of SLCV, the numbers of up- and downregulated genes were similar. Examining the functional classification of the genes (Table 1) suggests that the presence of begomoviruses, especially SLCV, in *B. tabaci*-induces genes related to mitochondrial respiration, metabolism, stress, and transport of macromolecules (Table 1). Interestingly, little overlap was observed between classes of genes that were significantly regulated in response to the two investigated begomoviruses.

The *hsp70* gene is overexpressed and results in higher HSP70 protein concentrations in viruliferous whiteflies. As observed in our microarray experiments, *hsp70* was overexpressed by more than 1.5-fold after acquisition and retention of TYLCV and SLCV (Fig. 2A). Interestingly, it is the only gene that was upregulated after uptake and retention of both viruses. This result was confirmed for TYLCV using a quantitative real-time RT-PCR approach, in which an overexpression of more than 1.7-fold was observed (Fig. 2A). The overexpression of *hsp70* was accompanied by an accumulation of HSP70 amounts with time as demonstrated by Western blot analysis, best seen 7 days after TYLCV acquisition (Fig. 2C). HSP70 accumulation was quantified 7 days after TYLCV acquisition relative to a tubulin control using the Scion Image densitometry software program, and the results showed an increase by 1.6-fold.

HSP70 Co-IP and interacts with TYLCV in virus overlay assays and immunocapture PCR. Following the overexpression of *hsp70* in response to TYLCV at the gene and protein levels, we tested whether this response involves direct interaction between TYLCV and the HSP70 protein. Three techniques were used to test this hypothesis. (i) Coimmuniprecipitation (Co-IP) of TYLCV coat protein (CP) with anti-HSP70 specific antibody and vice versa, to detect both proteins in crude extracts and to immunoprecipitate the other interacting protein. In both cases where anti-CP or anti-HSP70 antibodies were used for Co-IP, both antibodies coimmunoprecipitated the other interacting protein as detected by Western blotting, suggesting a specific interaction between CP and HSP70 (Fig. 3A and B). Control preimmune serums did not immunoprecipitate either protein, indicating the specific interaction between the two proteins (Fig. 3A and B). An additional control used was the GroEL protein produced by the endosymbiotic bacteria of *B. tabaci*, which was shown to interact with TYLCV CP (32). GroEL did not Co-IP with HSP70 (Fig. 3C), suggesting that the interaction between TYLCV CP and HSP70 is specific. (ii) Virus overlay protein binding assays (VOPBA) were performed to further validate the interaction of purified TYLCV virions and HSP70. HSP70 was detectable in the soluble and insoluble protein fractions of *B. tabaci* after Western blot analysis but in a

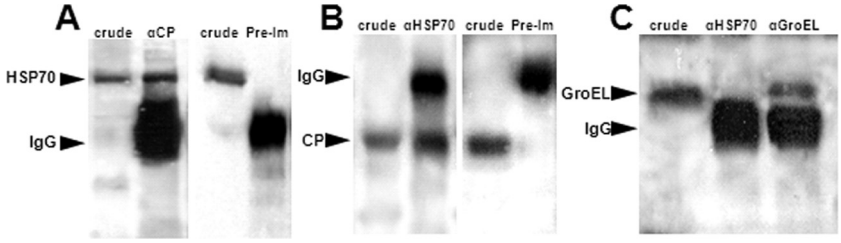

FIG 3 Coimmunoprecipitation of HSP70 and TYLCV CP with anti-TYLCV CP and anti-HSP70, respectively, in TYLCV viruliferous whitefly extracts. (A) Membranes reacted with anti-HSP70 antibody. HSP70 is detected in crude extracts and in extract incubated with protein A-Sepharose beads bound to anti-CP antibody but not in extract incubated with beads bound to preimmune serum (Pre-Im). (B) Membranes reacted with anti-TYLCV CP antibody. TYLCV CP is detected in crude extracts and in extract incubated with protein A-Sepharose beads bound to anti-HSP70 antibody but not in extract incubated with beads bound to preimmune serum. Both HSP70 and TYLCV CP proteins specifically coimmunoprecipitated with the other interacting protein. (C) Membrane is reacted with anti-GroEL antibody. GroEL is detected in whitefly crude extracts and in extracts incubated with protein A-Sepharose beads bound to anti-GroEL antibody, but HSP70 is not detected when protein A-Sepharose beads are bound to anti-HSP70. IgG molecules for confirming the presence of the antibodies in the membranes were also detected with the secondary antibody used.

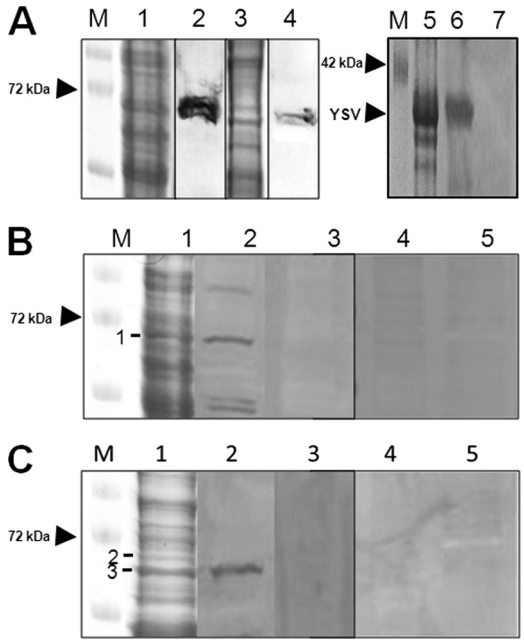

FIG 4 (A) Immunodetection of HSP70 in the soluble (lanes 1 and 2) and insoluble (lanes 3 and 4) protein fractions of *B. tabaci*. The proteins were subjected to SDS-PAGE (lanes 1 and 3), followed by Western analysis with anti-HSP70 antibodies (lanes 2 and 4). M, molecular weight marker. Immunodetection of purified YSV (15 μg protein per lane, lanes 5 and 6) and the soluble protein fraction of *B. tabaci* (120 μg protein per lane, lane 7) was done as a control. The proteins were subjected to SDS-PAGE (lane 5), followed by Western analysis with anti-YSV antibodies (DSMZ AS-517, 1 μg ml^{-1}; lanes 6 and 7). M, molecular weight marker. (B and C) Virus overlay protein binding assay with the soluble protein (B) or the insoluble protein fractions (C) of *B. tabaci*. After SDS-PAGE (lane 1), proteins were blotted and incubated with purified TYLCV virions (lane 2), purified YSV virions (lane 4), and buffer without virus (lanes 3 and 5). Virus binding was shown after application of primary antibodies against TYLCV (lanes 2 and 3) and YSV (lanes 4 and 5), secondary antibodies, and NBT-BCIP. M, molecular weight marker; band 1, heat shock protein 70; band 2, heat shock protein 70; for band 3, see Table 2.

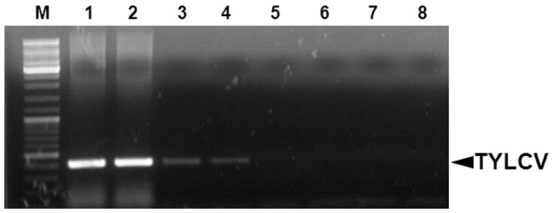

FIG 5 Immunocapture PCR assay to detect HSP70-TYLCV CP interaction in viruliferous whiteflies. A TYLCV-specific PCR product. as seen in lanes 1 and 2, was obtained when extracts of dissected midguts of viruliferous whiteflies were applied to PCR tubes coated with an anti-HSP70 specific antibody, and a PCR was performed on the caught complexes (lanes 3 and 4). Control treatments with midgut extracts of nonviruliferous whiteflies (lanes 5 and 6) and with uncoated tubes (lanes 7 and 8) were negative.

much lesser amount in the insoluble fraction (Fig. 4A). Virus binding to soluble and insoluble whitefly proteins was evaluated after protein separation, blotting, and incubation of the membranes with purified TYLCV virions with TYLCV-specific antibodies. Purified *Yam sphaerical aureus virus* (YSV) particles (a spherical virus detected with YSV-specific antibody from purified virions, as shown in Fig. 4A, lanes 5 and 6, that is not transmitted by or detected in *B. tabaci*, as shown in Fig. 4A, lane 7) and YSV-specific antibodies were applied to demonstrate the specificity of virus binding. TYLCV virions bound, among others, to a 70-kDa band of the soluble protein fraction shown by a prominent signal (Fig. 4B, lane 2, band 1). The main protein component of this band was identified as HSP70 (Table 2). No signal was detected for the 68-kDa band (Fig. 4C, lanes 1 and 2, band 2) of the insoluble protein fraction which also contained HSP70. In the insoluble protein fraction, a 65-kDa band containing a putative HSP70 band showed a strong signal (Fig. 4C, lanes 1 and 2, band 3). Unspecific binding of anti-TYLCV antibodies and secondary antibodies was never detected. In addition, YSV particles did not bind to any whitefly proteins, a result that points to a specific binding of the begomovirus particles and not to nonspecific stickiness of HSP70. (iii) The third assay used to validate the interaction between TYLCV and HSP70 was an immunocapture-PCR assay (IC-PCR). A TYLCV-specific PCR product similar to a positive control (Fig. 5, lanes 1 and 2) was obtained when extracts of viruliferous whiteflies were applied to PCR tubes coated with an HSP70-specific antibody and a sequential PCR was performed on the complexes bound to the antibody (Fig. 5, lanes 3 and 4). Negative TYLCV PCR results were obtained when extracts from nonviruliferous whiteflies or uncoated tubes were used as controls (Fig. 5, lanes 5 to 8), suggesting a specific interaction between HSP70 and TYLCV, very likely via the formation of HSP70 and TYLCV complexes.

HSP70 colocalizes with TYLCV and WmCSV in *B. tabaci* midgut. To follow the spatial distribution of HSP70 and TYLCV

TABLE 2 Analysis of protein bands that bound purified TYLCV virions in virus overlay protein binding assays[a]

Band	Identified protein	Accession no.	Theoretical mass (kDa)	Exptl mass (kDa)	Protein identification probability (%)	Coverage (%)
1	70-kDa heat shock protein, *Bemisia tabaci*	gi|156254075	71	70	100	60
2	70-kDa heat shock protein, *Bemisia tabaci*	gi|156254075	71	68	100	56
3	GI22533, *Drosophila mojavensis*	gi|193917024	68	65	100	7
	Hsp70, putative, *Ixodes scapularis*	gi|215501872	67	65	100	8
	GTP-binding protein LepA, *Rickettsia* endosymbiont of *Ixodes scapularis*	gi|239947763	67	65	100	5
	Similar to Igf2 mRNA binding protein, putative, *Nasonia vitripennis*	gi|156541968	64	65	100	7
	Similar to CG2812-PA, *Apis mellifera*	gi|110748705	64	65	100	4

[a] Protein bands were excised from corresponding Coomassie-stained gels and analyzed by electrospray ionization mass spectrometry. Peptide mass spectra were analyzed using the software program Scaffold3. Only proteins with an identification probability of 100%. are displayed. Numbering of the bands corresponds to the bands in Fig. 4.

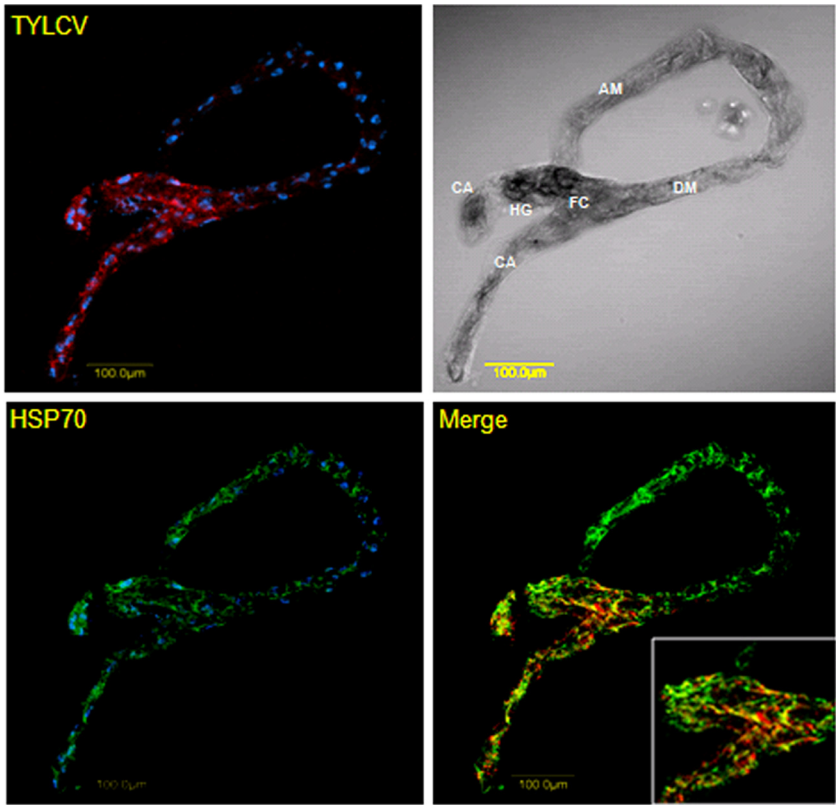

FIG 6 Colocalization of HSP70 and TYLCV in midguts of viruliferous whiteflies. HSP70 immunolocalization using specific first antibody and secondary antibody conjugated to Alexa Fluor (488 nm) (green) and TYLCV detection using a specific DNA probe conjugated to Cy3 (red). Note the yellow patches indicating colocalization of TYLCV and HSP70 in the filter chamber (FC) and cecae (CA) and the absence of TYLCV and colocalization signal in other parts of the midgut. Blue indicates DAPI staining of the nuclei. DM, descending midgut; AM, ascending midgut; HG, hindgut.

and their possible colocalization in whitefly midguts, we performed colocalization studies using an immunological detection of HSP70 and fluorescence *in situ* hybridization (FISH) or immunological detection of TYLCV and *Watermelon chlorotic stunt virus* (WmCSV) viral DNA in dissected midguts from viruliferous whiteflies. The highest TYLCV concentration shown by red fluorescence was found in the filter chamber and the cecae (Fig. 6, upper row), where HSP70 localization was also observed among the other parts of the midgut (lower row, green fluorescence). Colocalization of both HSP70 and TYLCV was clearly seen (Fig. 6, lower row merge) as yellow patches in the filter chamber and cecae, while no such signal was observed in other parts of the midgut. Colocalization of HSP70 and WmCSV was further observed in the ascending midgut (Fig. 7) when specific antibodies were used against WmCSV CP and HSP70, confirming the possible direct *in vivo* interaction between begomoviruses and HSP70.

Feeding whiteflies with anti-HSP70 antibody increases TYLCV transmission. Transmission experiments were performed with whiteflies fed with anti-HSP70 antibodies to further investigate the involvement of HSP70 in TYLCV transmission by *B. tabaci*. *B. tabaci* MEAM1 adults were first fed on artificial medium containing HSP70 antibodies and subsequently fed purified TYLCV virions. Whiteflies fed with preimmune serum instead of anti-HSP70 antibodies served as controls. Interestingly the transmission rates were enhanced, with 14 out of 24 plants in the first experiment and 23 out of 26 plants in the second experiment testing as being infected after feeding on anti-HSP70 antibodies, while only 10 out of 23 and 13 out of 25 plants tested as infected in the control experiments, in which whiteflies were fed with preimmune serum only. Altogether, 73% transmission rates, on average, were obtained after feeding with anti-HSP70 antibody, compared to 47% when the whiteflies were fed with preimmune serum (Fig. 8A), clearly demonstrating the involvement of HSP70 in virus transmission.

To demonstrate that HSP70 antibodies were internalized by the whiteflies, homogenates of insects previously fed on antibodies and insects fed on preimmune serum were used as the first antibody for the detection of HSP70 from whole whitefly protein extracts in Western analysis. While no signals were detectable after incubation of whitefly proteins with homogenates of insects previously fed on preimmune serum (Fig. 8B, lanes 3 and 4), faint signals were visible after application of homogenates of insects fed on anti-HSP70 antibodies, demonstrating the presence of the anti-HSP70 antibodies (Fig. 8B, lanes 1 and 2). Additionally, midguts were dissected from whiteflies fed on the first antibody against HSP70 or preimmune serum and subsequently fed on a goat-anti rabbit Alexa Fluor 568-nm secondary antibody. A clear signal was seen in the midguts from whiteflies fed with the HSP70 antibody, while no signal was observed in the control midgut dissected from whiteflies fed with preimmune serum (Fig. 8C).

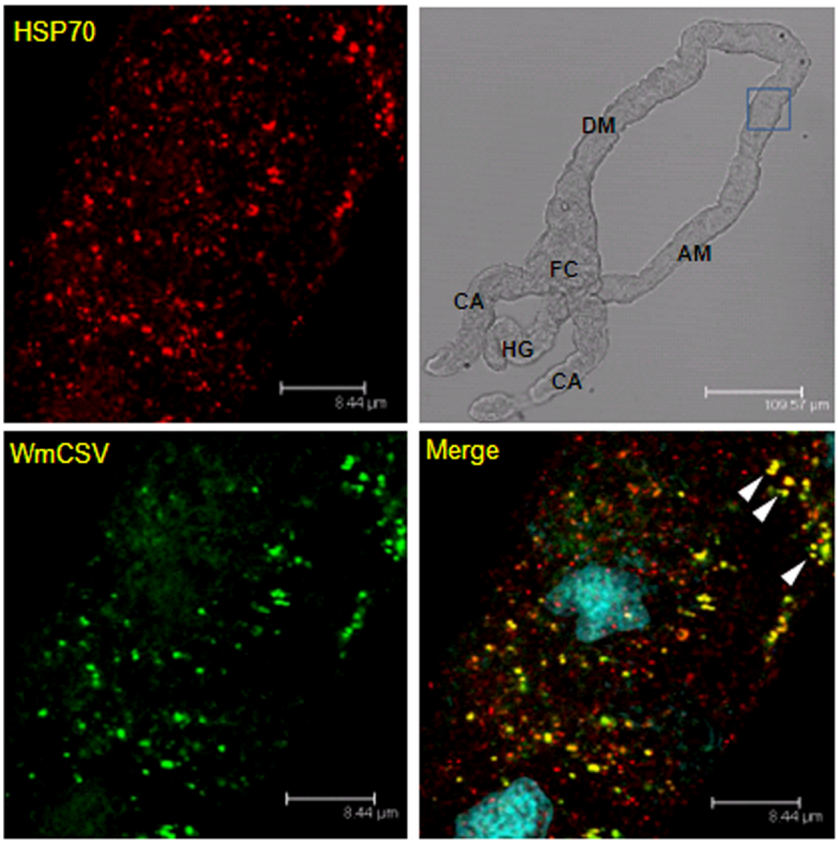

FIG 7 Colocalization of HSP70 and WmCSV in midguts of viruliferous whiteflies. HSP70 immunolocalization using specific first antibody and secondary antibody conjugated to Alexa Fluor (635 nm) (red) and WmCSV immunolocalization using specific first antibody and secondary antibody conjugated to Alexa Fluor (488 nm) (green). Note the yellow areas indicating colocalization of WmCSV and HSP70 in the ascending midgut (AM). Blue indicates DAPI staining of the nuclei. DM, descending midgut; CA, cecae; HG, hindgut; FC, filter chamber.

DISCUSSION

We have performed microarray experiments to investigate the response of *B. tabaci* to the presence of the Old World monopartite TYLCV and the New World bipartite SLCV. A low number of genes responded to the uptake and retention of TYLCV in the whitefly. In comparison, a higher number of genes were significantly regulated after the uptake of SLCV. This difference in the response is likely related to the coevolution between the Old World *B. tabaci* MEAM1 with the Old World TYLCV begomovirus, which is well adapted to the whitefly and to a lower compatibility with the New World SLCV (9, 16). The transcriptional changes are likely to be related to virus interaction with insect organs and not the feeding on the infected plants. This is because the setup of the experiment included rearing the viruliferous and nonviruliferous whiteflies used for RNA extraction on TYLCV-nonhost cotton plants for sufficient time to prevent residual effects from the infected plant. Genes that were differently expressed due to virus uptake were involved in several biological processes, including stress response, macromolecule transport, metabolism, and mitochondrial functions, as already shown for TYLCCV by Luan et al. (47). Remarkably, the genes significantly regulated in response to TYLCV and SLCV were significantly different, suggesting a differential response to the acquisition and retention of these two viruses that belong to the same genus. Only one gene was significantly upregulated in response to both TYLCV and SLCV. This gene encodes the stress-related heat shock protein 70 (*hsp70*). The elevated expression of *hsp70* was confirmed using a qRT-PCR approach (Fig. 2). Interestingly, *hsp70* was upregulated at the same order of magnitude after the uptake of *Watermelon chlorotic stunt virus* (WmCSV), another whitefly-transmitted begomovirus (data not shown). The upregulation of *hsp70* resulted in elevated concentrations of the heat shock protein HSP70 as demonstrated by Western blot analysis (Fig. 2). The specificity of the upregulation of *hsp70* in response to begomoviruses was further confirmed by performing a control experiment in which the expression of the *hsp70* gene was analyzed 2 and 9 days after the uptake of *Faba bean necrotic stunt virus*, an aphid-transmitted virus which is not transmitted by *B. tabaci*. The results showed that the expression of *hsp70* was not enhanced (data not shown). This result demonstrates that the uptake of different begomoviruses that are transmitted by *B. tabaci* results in *hsp70* upregulation, while no upregulation is observed when a virus that is not transmitted by *B. tabaci* is acquired.

HSP70 is ubiquitously expressed, with unusually high conservation in protein sequence and functional features (6, 42), and the functions are well established (23, 34, 35, 53). HSPs and their constitutively synthesized relatives known as heat shock cognates or HSC proteins belong to a multicomponent and multifunctional chaperone family that plays a role in various cellular processes, such as disaggregation of proteins from large aggregates or

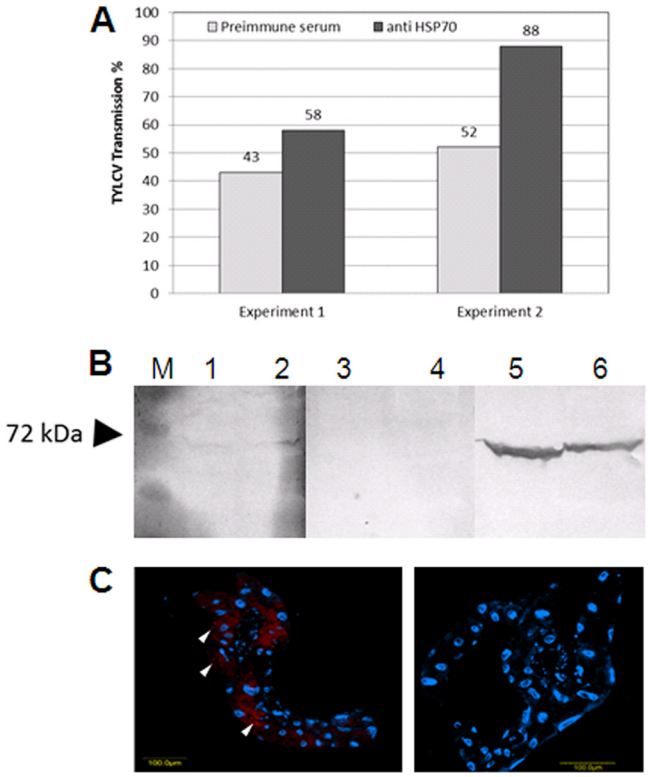

FIG 8 (A) Enhancement of TYLCV transmission rates after feeding of whiteflies on artificial medium containing anti-HSP70 antibodies and preimmune serum, respectively, for 1 day followed by feeding on the same medium containing purified TYLCV virions for another day. (B) Detection of ingested HSP70 antibodies in whiteflies fed on artificial medium containing anti-HSP70 antibodies for 2 days. The soluble (lanes 1, 3, and 5) and insoluble (lanes 2, 4, and 6) protein fractions of *B. tabaci* were subjected to SDS-PAGE and blotting followed by immunodetection of HSP70. Homogenates of whiteflies fed on artificial medium amended with anti-HSP70 antibodies (lanes 1 and 2) and preimmune serum (lanes 3 and 4) were used as a source for HSP70 antibodies. HSP70 antibodies were used as a positive control (lanes 5 and 6). (C) Detection of ingested HSP70 antibodies in the midgut after feeding with anti-HSP70 first antibody for 24 h (left) or with preimmune serum (right) and subsequently feeding with a goat antirabbit Alexa Fluor 568-nm secondary antibody for another 24 h. M, molecular weight marker.

assemblies, prevention of aggregation of denatured proteins, aiding of the renaturation or folding of proteins to reach their proper conformation, direction of proteins to degradative pathways, and binding of proteins to restrain their function, making them available for ligand binding or allowing them to translocate across membranes. Although some of the classes of HSPs clearly have distinct activities, they also exhibit overlapping functions and may share proteins that act as cofactors, known as cochaperones (41, 46, 65, 72). Extracellular and membrane-bound HSPs are involved in immunological functions (58, 61). Previous findings have implicated members of the HSP70 family in the targeted transport of proteins to specific cellular domains (66, 67, 75). Furthermore, HSP70s were shown to play various roles in the life cycles of plant and animal viruses (33, 74). Some plant viruses, such as closteroviruses, encode their own HSP70 homolog, which, in combination with the virus coat protein, facilitates transport through plasmodesmata and thus enables cell-to-cell movement (1, 2, 54). In tombusviruses, cytosolic HSP70s play multiple roles in *Tomato bushy stunt virus* (TBSV) replication, such as affecting the subcellular localization and membrane insertion of the viral replication proteins, as well as the assembly of the viral replicase (79). Krenz et al. (43) showed a targeted transport of *Abutilon mosaic virus* movement protein toward the chloroplasts shuttled by a heat shock cognate 70-kDa protein. For several animal viruses, the interaction with HSP70s appears to be involved in virion assembly, which may take place in the cytoplasm, nucleus, or endoplasmatic reticulum depending on the requirements of different viruses (15, 45). Oh & Song (63) demonstrated an interaction of the coat protein of *West Nile virus* (*Flavivirus*) with HSP70 using the yeast two-hybrid system and purified proteins. Couturier et al. (14) found high-affinity binding between an inducible HSP70 and the measles virus nucleoprotein (which requires an HSP40 cochaperone). In most cases, HSP70 displays stability and activity control reactions, and binding to HSP70 results in enhanced transcription and replication of these viruses. For animal viruses, HSP70 promotes gene expression for several viral families (12), e.g., for baculoviruses (49). An involvement of HSP70 in viral cell-to-cell transport has not yet been reported for animal cells. The role of HSP70 in interaction of plant viruses with their vector insects is unknown as well.

Enhanced *hsp70* expression and elevated HSP70 concentrations were found especially within the filter chamber, where the largest amounts of the virus were detected by *in situ* hybridization and immunolocalization (25, 26; also unpublished data). These results are supported by previous observations that the majority of TYLCV particles are translocated from the filter chamber into the hemolymph (25, 26, 71). Colocalization of TYLCV and HSP70 was mainly observed in the filter chamber; however, colocalization was also observed in other parts of the midgut. These results were confirmed by immunolocalization studies with the bipartite WmCSV and HSP70 that resulted in high colocalization rates. These results point to a direct interaction *in vivo*. To validate this interaction, further experiments are required to visualize this interaction at a higher resolution level: for instance, using transmission electron microscopy and immunolabeling.

All results indicate a direct or indirect response of whiteflies to begomovirus uptake. Several experiments we performed, including Co-IP (Fig. 3), VOPBA (Fig. 4), and IC-PCR (Fig. 5), proved the possibility of binding of HSP70 and TYLCV *in vitro*. In addition, HSP70 and virions were to some extend colocalized in the filter chamber and the ascending midgut, pointing to a direct interaction *in vivo* (Fig. 6 and 7). One possible role of HSP70 could be the aided/directed shuttling of the TYLCV virions through the insect midgut cells to the hemolymph, thus minimizing virus contact with insect tissue. In this case, the insect promotes virus transmission to minimize harmful effects caused by the virus, which was previously shown to cause negative effects to the insect, including a decrease in the longevity and fecundity of viruliferous whiteflies (17, 68). A previous study showed the binding of TYLCV particles to the chaperone GroEL, which is produced by *Hamiltonella*, a secondary symbiont of *B. tabaci*, thus supporting the hypothesis that proteins produced within the vector aid in virus transmission (32). Following this hypothesis, one would expect reduced virus transmission after blocking HSP70 by feeding HSP70 antibodies to the whiteflies. In contrast to these expectations, TYLCV transmission was enhanced after anti-HSP70 antibody uptake (Fig. 8). The enhanced transmission is not a result of uptake of proteins that stabilize virus particles, as hypothesized by Bencharki et al. (5), who found stimulated transmission of virus

by aphids after uptake of several soluble proteins, because feeding *B. tabaci* with bovine serum albumin and anti-WmCSV antibodies (DSMZ AS830) did not result in higher transmission rates for TYLCV (data not shown). Since TYLCV was shown to cause negative effects on *B. tabaci*, the overexpression of HSP70 at the gene and protein levels could result from a stress or immune response of the vector in response to the virus. In other species, such as leafminers (38), *Drosophila* (73, 80), and even desert lizards (76, 81), the inductive and conserved role of HSP70 in the stress response is well documented. The overexpression of *hsp70* in response to stress was reported for mammalian systems with autoimmune disorders, supporting the possibility that overexpression of *hsp* contributes to immunopathological changes (82). The overexpression of *hsp70* might be direct, by recognizing the presence of the virus, or indirect, through a conserved stress response pathway. The heat shock protein response, although related to heat, can also be related to other stresses, such as infection, inflammation, radiation, hypoxia, and chemical stressors (50). The ability of *B. tabaci* to respond to the presence of begomoviruses and other invaders was previously documented for a number of invaders, including begomoviruses (47) and parasitoids (52). These responses were related to several stress response pathways, such as the Toll-like, Imd, and mitogen-activated protein kinase (MAPK)-related pathways in the case begomoviruses and parasitoids and heat shock, mitochondrial, and cytoskeleton-related genes in the case of heat stress (51).

The transcriptional response of *hsp70* activation starts in the cytoplasm with trimerization of heat shock factors (HSF) that enter the nucleus and bind to the heat shock elements (HSE) on the DNA (69). HSFs are the first molecules to sense the stress and respond accordingly, and thus it is likely that HSFs sense the presence of the high concentration of TYLCV virions in the cytoplasm of the cell. The function of HSP70 as a refolder and stabilizer of proteins through direct interaction with them suggests possible binding to TYLCV particles in the cell cytoplasm, as observed in our results (Fig. 6 and 7). Since a main function for HSP70 is selectively targeting cytosolic proteins to lysosomes for degradation, it is likely that interaction with TYLCV particles might be a protective response for degrading TYLCV virions. The results of the feeding experiments support this hypothesis. Uptake of anti-HSP70 antibodies into the midgut was proven by using extracts of fed and discharged whiteflies as antibodies for HSP70 in Western blot analysis and by localization after confocal laser scanning microscopy (CLSM) (Fig. 8). The enhanced TYLCV transmission rates after feeding on HSP70 antibodies suggest an inhibition of HSP70-virus interaction/binding and presenting them for degradation. Thus, more TYLCV virions could pass the midgut barrier and enter the hemolymph; still, further experiments have to be conducted to confirm this hypothesis.

ACKNOWLEDGMENTS

This research was supported by research grant no. 908-42.12/2006 from the German-Israeli Foundation (GIF) to S.W., H.C., and M.G. and grant no. IS-4062-07 from the United States-Israel Binational Agricultural Research and Development Fund (BARD) to M.G., H.C., and J.K.B. and in part by an Israel Science Foundation research grant, no. 884/07, to M.G. and H.C.

We thank Henning Urlaub (Bioanalytical Mass Spectrometry, Max Planck Institute for Biophysical Chemistry, Göttingen, Germany) for analyzing proteins using LC-ESI-MS.

REFERENCES

1. **Alzhanova DV, Napuli AJ, Creamer R, Dolja VV.** 2001. Cell-to-cell movement and assembly of a plant closterovirus: roles for the capsid proteins and Hsp70 homolog. EMBO J. **20**:6997–7007.
2. **Aoki K, Kragler F, Xoconostle-Cazares B, Lucas WJ.** 2002. A subclass of plant heat shock cognate 70 chaperones carries a motif that facilitates trafficking through plasmodesmata. Proc. Natl. Acad. Sci. U. S. A. **99**: 16342–16347.
3. **Azzam O, et al.** 1994. Whitefly transmission and efficient ssDNA accumulation of bean golden mosaic geminivirus require functional coat protein. Virology **204**:289–296.
4. **Baugh LR, Hill AA, Brown EL, Hunter CP.** 2001. Quantitative analysis of mRNA amplification by in vitro transcription. Nucleic Acids Res. **29**: E29. doi:10.1093/nar/29.5.e29.
5. **Bencharki B, et al.** 2010. Phloem protein Partners of Cucurbit aphid borne yellows virus: possible involvement of phloem proteins in virus transmission by aphids. Mol. Plant Microbe Interact. **23**:799–810.
6. **Boorstein WR, Ziegelhoffer T, Craig EA.** 1994. Molecular evolution of the HSP70 multigene family. J. Mol. Evol. **38**:1–17.
7. **Bosco D, Mason G, Accotto GP.** 2004. TYLCSV DNA, but not infectivity, can be transovarially inherited by the progeny of the whitefly vector *Bemisia tabaci* (Gennadius). Virology **323**:276–283.
8. **Briddon RW, Pinner MS, Stanley J, Markham PG.** 1990. Geminivirus coat protein gene replacement alters insect specificity. Virology **177**: 85–94.
9. **Brown JK.** 2010. Phylogenetic biology of the Bemisia tabaci sibling species group, p 31–67. *In* Stansley PA, Naranjo SE (ed), Bemisia: bionomics and management of a global pest. Springer, New York, NY.
10. **Brown JK, Czosnek H.** 2002. Whitefly transmission of plant viruses, p 65–100. *In* Plumb RT (ed), Advances in botanical research, vol 36: plant virus vector interactions. Academic Press, New York, NY.
11. **Caciagli P, Bosco D.** 1997. Quantitation over time of tomato yellow leaf curl geminivirus DNA in its whitefly vector. Phytopathology **87**: 610–613.
12. **Carsillo T, et al.** 2009. Major histocompatibility complex haplotype determines hsp70-dependent protection against measles virus neurovirulence. J. Virol. **83**:5544–5555.
13. **Cicero JM, Hiebert E, Webb SE.** 1995. The alimentary canal of *Bemisia tabaci* and *Trialeurodes abutilonea* (Homoptera, Sternorrhynchi): histology, ultrastructure and correlation to function. Zoomorphology **115**:31–39.
14. **Couturier M, et al.** 2010. High affinity binding between Hsp70 and the C-terminal domain of the measles virus nucleoprotein requires an Hsp40 co-chaperone. J. Mol. Recognit. **23**:301–315.
15. **Cripe TP, Delos SE, Estes PA, Garcea RL.** 1995. In vivo and in vitro association of hsc70 with polyomavirus capsid proteins. J. Virol. **69**:7807–7813.
16. **Czosnek H, Ghanim M, Ghanim M.** 2002. Circulative pathway of begomoviruses in the whitefly vector *Bemisia tabaci*—insights from studies with *Tomato yellow leaf curl virus*. Ann. Appl. Biol. **140**:215–231.
17. **Czosnek H, et al.** 2001. Whiteflies: vectors—or victims?—of geminiviruses, p 291–322. *In* Maramorosch K (ed), Advances in virus research, vol 57. Academic Press, New York, NY.
18. **Czosnek H, Laterrot H.** 1997. A worldwide survey of tomato yellow leaf curl viruses. Arch. Virol. **142**:1391–1406.
19. **De Barro PJ, Liu SS, Boykin LM, Dinsdale AB.** 2011. *Bemisia tabaci*: a statement of species status. Annu. Rev. Entomol. **56**:1–19.
20. **Dellaporta S, Wood J, Hicks JB.** 1983. A plant DNA minipreparation: version II. Plant Mol. Biol. Rep. **1**:19–21.
21. **Dinsdale A, Cook L, Riginos C, Buckley YM, De Barro P.** 2010. Refined global analysis of *Bemisia tabaci* (Hemiptera: Sternorrhyncha: Aleyroidae: Aleyrodidae) mitochondrial cytochrome oxidase 1 to identify species level genetic boundaries. Ann. Entomol. Soc. Am. **103**:196–208.
22. Reference deleted.
23. **Flynn GC, Pohl J, Flocco MT, Rothman JE.** 1991. Peptide-binding specificity of the molecular chaperone BiP. Nature **353**:726–730.
24. **Frohlich D, Torres-Jerez I, Bedford ID, Markham PG, Brown JK.** 1999. A phylogeographic analysis of the *Bemisia tabaci* species complex based on mitochondrial DNA markers. Mol. Ecol. **8**:1683–1691.
25. **Ghanim M, Brumin M, Popovski S.** 2009. A simple, rapid and inexpensive method for localization of *Tomato yellow leaf curl virus* and

Potato leafroll virus in plant and insect vectors. J. Virol. Methods **159**: 311–314.
26. **Ghanim M, Medina V.** 2007. Localization of Tomato yellow leaf curl virus in its whitefly vector Bemisia tabaci, p 171–183. *In* Czosnek H (ed), Tomato yellow leaf curl virus disease. Springer, Dordrecht, The Netherlands.
27. Reference deleted.
28. **Ghanim M, Morin S, Czosnek H.** 2001. Rate of *Tomato Yellow Leaf Curl Virus* (TYLCV) translocation in the circulative transmission pathway of its vector, the whitefly *Bemisia tabaci.* Phytopathology **91**:188–196.
29. **Ghanim M, et al.** 2001. Microscopic analysis of the digestive, salivary and reproductive organs of *Bemisia tabaci* (Gennadius) (Hemiptera: Aleyrodidae) biotype B. J. Morphol. **248**:22–40.
30. **Ghanim M, Czosnek H.** 2000. *Tomato yellow leaf curl geminivirus* (TYLCV-Is) is transmitted among whiteflies (*Bemisia tabaci*) in a sex-related manner. J. Virol. **74**:4738–4745.
31. **Ghanim M, Morin S, Zeidan M, Czosnek H.** 1998. Evidence for transovarial transmission of tomato yellow leaf curl virus by its vector the whitefly *Bemisia tabaci.* Virology **240**:295–303.
32. **Gottlieb Y, et al.** 2010. The transmission efficiency of Tomato yellow leaf curl virus is correlated with the presence of a specific symbiotic bacterium species. J. Virol. **84**:9310–9317.
33. **Hafren A, Hofius D, Rönnholm G, Sonnewald U, Makinen K.** 2010. HSP70 and its cochaperone CPIP promote potyvirus infection in *Nicotiana benthamiana* by regulating viral coat protein functions. Plant Cell **22**:523–535.
34. **Hartl FU, Hayer-Hartl M.** 2002. Molecular chaperones in the cytosol: from nascent chain to folded protein. Science **295**:1852–1858.
35. **Hartl FU.** 1996. Molecular chaperones in cellular protein folding. Nature **381**:571–579.
36. **Hofer P, Bedford ID, Markham PG, Jeske H, Frischmuth T.** 1997. Coat protein gene replacement results in whitefly transmission of an insect nontransmissible geminivirus isolate. Virology **236**:288–295.
37. **Hogenhout SA, van der Wilk F, Verbeek M, Goldbach RW, van den Heuvel JFJM.** 1998. Potato leafroll virus binds to the equatorial domain of the aphid endosymbiotic GroEL homologue. J. Virol. **72**:358–365.
38. **Huang LH, Kang L.** 2007. Cloning and interspecific altered expression of heat shock protein genes in two leafminer species in response to thermal stress. Insect Mol. Biol. **16**:491–500.
39. **Hunter WB, Hiebert E, Webb SE, Tsai JH, Polston JE.** 1998. Location of geminiviruses in the whitefly *Bemisia tabaci* (Homoptera: Aleyrodidae). Plant Dis. **82**:1147–1151.
40. **Jiu M, et al.** 2007. Vector-virus mutualism accelerates population increase of an invasive whitefly. PLoS One **2**:e182. doi:10.1371/journal.pone.0000182.
41. **Johnston JA, Ward CL, Kopito RR.** 1998. Aggresomes: a cellular response to misfolded proteins. J. Cell Biol. **143**:1883–1898.
42. **Karlin S, Brocchieri L.** 1998. Heat shock protein 70 family: multiple sequence comparisons function and evolution. J. Mol. Evol. **47**:565–577.
43. **Krenz B, Windeisen V, Wege C, Jeske H, Kleinow T.** 2010. A plastid-targeted heat shock cognate 70 kDa protein interacts with the *Abutilon mosaic virus* movement protein. Virology **401**:6–17.
44. Reference deleted.
45. **Liberman E, et al.** 1999. Activation of the grp78 and grp94 promoters by hepatitis C virus E2 envelope protein. J. Virol. **73**:3718–3722.
46. **Lindquist SL.** 1986. The heat-shock response. Annu. Rev. Biochem. **55**: 1151–1191.
47. **Luan JB, et al.** 2011. Global analysis of the transcriptional response of whitefly to *Tomato yellow leaf curl china virus* reveals their relationship of coevolved adaptations. J. Virol. **85**:3330–3340.
48. Reference deleted.
49. **Lyupina YV, et al.** 2010. An important role of the heat shock response in infected cells for replication of baculoviruses. Virology **406**:336–341.
50. **Macario AJ, de Macario EC.** 2000. Stress and molecular chaperones in disease. Int. J. Clin. Lab Res. **30**:49–66.
51. **Mahadav A, Kontsedalov S, Czosnek H, Ghanim M.** 2009. Thermotolerance and gene expression following heat stress in the whitefly *Bemisia tabaci* B and Q. biotypes. Insect Biochem. Mol. Biol. **39**:668–676.
52. **Mahadav A, Gerling D, Gottlieb Y, Czosnek H, Ghanim M.** 2008. Parasitization by the wasp *Eretmocerus mundus* induces transcription of genes related to immune response and symbiotic bacteria proliferation in the whitefly *Bemisia tabaci.* BMC Genomics **9**:342. doi:10.1186/1471-2164-9-342.
53. **Mayer MP.** 2005. Recruitment of Hsp70 chaperones: a crucial part of viral survival strategies. Rev. Physiol. Biochem. Pharmacol. **153**:1–46.
54. **MedinaV Peremyslov VV, Hagiwara Y, Dolja VV.** 1999. Subcellular localization of the HSP70-homolog encoded by beet yellows closterovirus. Virology **260**:173–181.
55. **Mehta P, Wyman JA, Nakhla MK, Maxwell DP.** 1994. Transmission of tomato yellow leaf curl geminivirus by *Bemisia tabaci* (Homoptera: Aleyrodidae). J. Ecol. Entomol. **87**:1291–1297.
56. **Morin S, Ghanim M, Sobol I, Czosnek H.** 2000. The GroEL protein of the whitefly *Bemisia tabaci* interacts with the coat protein of transmissible and non-transmissible begomoviruses in the yeast two-hybrid system. Virology **276**:404–416.
57. **Morin S, et al.** 1999. A GroEL homologue from endosymbiotic bacteria of the whitefly *Bemisia tabaci* is implicated in the circulative transmission of *Tomato yellow leaf curl virus.* Virology **30**:75–84.
58. **Multhoff G.** 2007. Heat shock protein 70 (Hsp70): membrane location, export and immunological relevance. Methods **43**:229–237.
59. Reference deleted.
60. Reference deleted.
61. **Nishikawa M, Takemoto S, Dakakura Y.** 2008. Heat shock protein derivatives for delivery of antigens to antigen presenting cells. Int. J. Pharm. **354**:23–27.
62. **Noris E, et al.** 1998. Amino acids in the capsid protein of tomato yellow leaf curl virus that are crucial for systemic infection, particle formation, and insect transmission. J. Virol. **72**:10050–10057.
63. **Oh W, Song J.** 2006. Hsp70 functions as a negative regulator of West Nile virus capsid protein through direct interaction. Biochem. Biophys. Res. Commun. **347**:994–1000.
64. **Ohnesorge S, Bejarano ER.** 2009. Begomovirus coat protein interacts with a small heatshock protein of its transmission vector (*Bemisia tabaci*). Insect Mol. Biol. **18**:693–703.
65. **Pelham HR.** 1986. Speculations on the functions of the major heat shock and glucose-regulated proteins. Cell **46**:959–961.
66. **Pishvaee B, et al.** 2000. A yeast DNA J protein required for uncoating of clathrin-coated vesicles in vivo. Nat. Cell Biol. **2**:958–963.
67. **Pratt WB, Silverstein AM, Galigniana MD.** 1999. A model for the cytoplasmic trafficking of signalling proteins involving the hsp90-binding immunophilins and p50. Cell Signal. **11**:839–851.
68. **Rubinstein G, Czosnek H.** 1997. Long-term association of tomato yellow leaf curl virus (TYLCV) with its whitefly vector *Bemisia tabaci*: effect on the insect transmission capacity, longevity and fecundity. J. Gen. Virol. **78**:2683–2689.
69. **Sarge KD, Murphy SP, Morimoto RI.** 1993. Activation of heat shock gene transcription by heat shock factor 1 involves oligomerization, acquisition of DNA-binding activity, and nuclear localization and can occur in the absence of stress. Mol. Cell. Biol. **13**:1392–1407.
70. **Sinisterra XH, McKenzie CL, Hunter WB, Powell CA, Shatters RG, Jr.** 2005. Differential transcriptional activity of plant-pathogenic begomoviruses in their whitefly vector (*Bemisia tabaci*, Gennadius: Hemiptera Aleyrodidae). J. Gen. Virol. **86**:1525–1532.
71. **Skaljac M, Ghanim M.** 2010. *Tomato yellow leaf curl virus* and the plant-virus-vector interactions. Isr. J. Plant Sci. **58**:103–111.
72. **Sorensen JG, Kristensen GTN, Loeschcke V.** 2003. The evolutionary and ecological role of heat shock proteins. Ecol. Lett. **6**:1025–1037.
73. **Sorensen JG, Dahlgaard J, Loeschcke V.** 2001. Genetic variation in thermal tolerance among natural populations of Drosophila buzzatii: down regulation of HSP70 expression and variation in heat-stress resistance traits. Funct. Ecol. **15**:289–296.
74. **Sullivan CS, Pipas JM.** 2001. The virus-chaperone connection. Virology. **287**:1–8.
75. **Tsai MY, Morfini G, Szebenyi G, Brady ST.** 2000. Release of kinesin from vesicles by hsc70 and regulation of fast axonal transport. Mol. Biol. Cell **11**:2161–2173.
76. **Ulmasov KA, Shammakov S, Karaev K, Evgenev MB.** 1992. Heat-shock proteins and thermoresistance in lizards. Proc. Natl. Acad. Sci. U. S. A. **89**:1666–1670.
77. **van den Heuvel JFJM, Verbeek M, van der Wilk F.** 1994. Endosymbiotic bacteria associated with circulative transmission of *potato leafroll virus* by *Myzus persicae.* J. Gen. Virol. **75**:2559–2565.
78. **van den Heuvel JFJM, et al.** 1997. The N-terminal region of the luteovirus readthrough domain determines virus binding to *Buchnera* GroEL and is essential for virus persistence in the aphid. J. Virol. **71**: 7258–7265.

79. **Wang RY, Stork J, Pogany J, Nagy PD.** 2009. A temperature sensitive mutant of heat shock protein 70 reveals an essential role during the early steps of tombusvirus replication. Virology **394**:28–38.
80. **Zatsepina OG, et al.** 2001. A Drosophila melanogaster strain from subequatorial Africa has exceptional thermotolerance but decreased HSP70 expression. J. Exp. Biol. **204**:1869–1881.
81. **Zatsepina OG, et al.** 2000. Thermotolerant desert lizards characteristically differ in terms of heat-shock system regulation. J. Exp. Biol. **203**: 1017–1025.
82. **Zugel U, Kaufmann SH.** 1999. Role of heat shock proteins in protection from and pathogenesis of infectious diseases. Clin. Microbiol. Rev. **12**: 19–39.